Pet. Sci. (2015) 12:232–251
DOI 10.1007/s12182-015-0027-8

ORIGINAL PAPER

Sequence stratigraphy of the petroliferous Dariyan Formation (Aptian) in Qeshm Island and offshore (southern Iran)

P. Mansouri-Daneshvar[1] · R. Moussavi-Harami[1] · A. Mahboubi[1] · M. H. M. Gharaie[1] · A. Feizie[2]

Received: 24 June 2014 / Published online: 7 April 2015

Abstract After sea level rises during the Early Cretaceous, upper parts of the Khami Group sediments (Fahliyan, Gadvan, and Dariyan Formations) deposited over Jurassic sediments. The Lower Cretaceous (Aptian) Dariyan Formation (equivalent to the Shu'aiba Formation and Hawar Member of the Arabian Plate) carbonates, which have hydrocarbon reservoir potential, form the uppermost portion of the Khami Group that unconformably overlays the Gadvan Formation and was unconformably covered by the Kazhdumi Formation and Burgan sandstones. Detailed paleontological, sedimentological, and well log analysis were performed on seven wells from Qeshm Island and offshore in order to analyze the sequence stratigraphy of this interval and correlate with other studies of the Dariyan Formation in this region. According to this study, the Dariyan Formation contains 14 carbonate lithofacies, which deposited on a ramp system that deepened in both directions (NE—wells 5, 6 and SW—wells 1, 2). Sequence stratigraphy led to recognition of 5 Aptian third-order sequences toward the Bab Basin (SW—well 1) and 4 Aptian third-order sequences toward Qeshm Island (NE—wells 5 and 6) so these areas show higher gamma on the gamma ray logs and probably have higher source rock potential. Other wells (wells 2–4 and 7) mainly deposited in shallower ramp systems and contain 3 Aptian third-order sequences. On the other hand, rudstone and boundstone lithofacies of studied wells have higher reservoir potential and were deposited during Apt 3 and Apt 4 sequences of the Arabian Plate. The Dariyan Formation in Qeshm Island (well 6) and adjacent well (well 5) was deposited in an intrashelf basin that should be classified as a new intrashelf basin in future Aptian paleogeographic maps. We interpret that salt-related differential subsidence, crustal warping, and reactivation of basement faults of the Arabian Plate boundary were responsible for the creation of the intrashelf basin in the Qeshm area.

Keywords Arabian Plate · Sequence stratigraphy · Qeshm Island · Aptian and Dariyan formation

1 Introduction

The Persian Gulf contains 55–68 % of the world's recoverable oil and more than 40 % of gas reserves (Konyuhov and Maleki 2006). Cretaceous carbonate platforms encompass approximately 16 % of world's hydrocarbon reservoirs developed in the Tethyan region including the Persian Gulf (Scott et al. 1993). The Lower Cretaceous (Aptian) Dariyan Formation comprises the uppermost portion of the Upper Jurassic to Lower Cretaceous Khami Group (James and Wynd 1965). This formation is predominantly composed of limestones deposited on a passive margin (Sharland et al. 2001) and its upper part is equivalent to the Shu'aiba Formation in the Arabian Plate region. In the Arabian Plate, the Hawar Member and Shu'aiba Formation (in this study both equivalent to the Dariyan Formation) unconformably overlay the Kharaib Formation (in this study equivalent to the Gadvan Formation) and were unconformably covered by the Nahr Umr

✉ P. Mansouri-Daneshvar
p.mansouri.daneshvar@gmail.com

[1] Department of Geology, Faculty of Sciences, Ferdowsi University of Mashhad, Mashhad, Iran

[2] Exploration Directorate, National Iranian Oil Company, Tehran, Iran

Edited by Jie Hao

Formation (equivalent to the Kazhdumi Formation) and Burgan sandstones after relative sea-level fall resulting in exposure of the platform with a strong diachronous boundary (Van Buchem et al. 2010b; Motiei 1993) (Fig. 1).

The Dariyan Formation has potential for hydrocarbon reservoirs and produced oil from the Alpha and Reshadat (Raksh) fields, and oil and gas in the Resalat (Rostam) Field (Alsharhan and Nairn 1997). Because of the

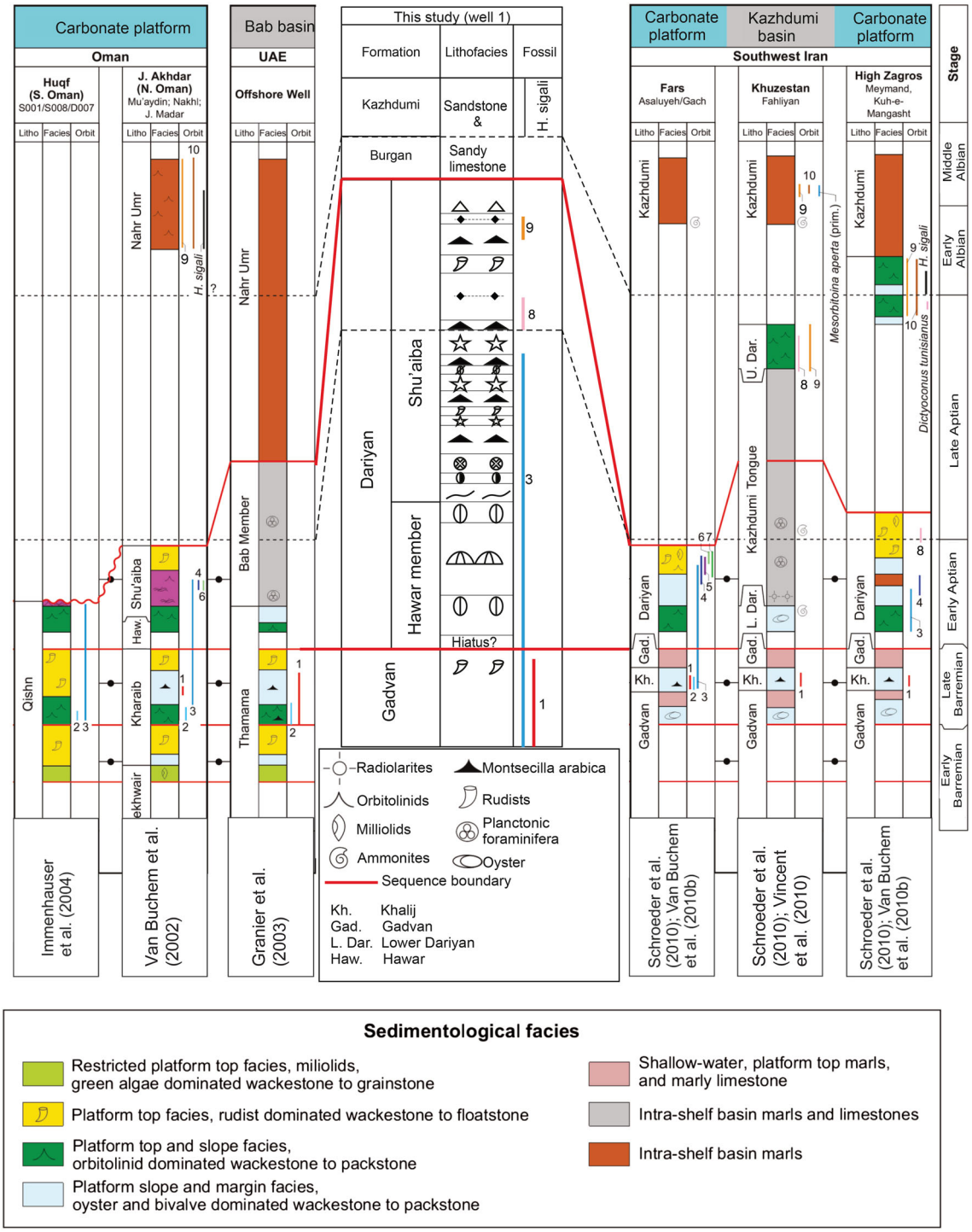

Fig. 1 Chronostratigraphy of the Barremian–Aptian with the orbitolinid distribution in the southern Arabian Plate (Oman, UAE, southwest Iran) (after Schroeder et al. 2010) that correlated with well 1 of this study, *1 Montseciella arabica*, *2 Eopalorbitolina transiens*, *3 Palorbitolina lenticularis*, *4 Palorbitolina ultima*, *5 Palorbitolinoides cf. orbiculata*, *6 Palorbitolina cormy*, *7 Palorbitolina wienandsi*, *8 Mesorbitolina parva*, *9 Mesorbitolina texana*, *10 Mesorbitolina subconcava*, for lithofacies symbols of this study see Fig. 5

importance of such reservoirs, sequence stratigraphic studies can play a significant role in reservoir studies and access its connectivity around the study area (Ainsworth 2006; Van Wagoner et al. 1988). Van Buchem et al. (2010b) and Vincent et al. (2010) proposed a new sequence stratigraphic framework for the Gadvan, Dariyan, and Kazhdumi Formations in SW Iran but there is no detailed work in the Iranian part of the Persian Gulf and no correlations performed with adjacent Arabian parts according to log data. The objectives of this study are to interpret depositional sequences by collecting petrographical studies of cores, cuttings, and log data and correlation of sequences between the Iranian part and the Arabian Plate in a vast area of Qeshm Island and offshore in southern Iran (eastern Persian Gulf) (Fig. 2) that can give a better clue in paleogeography during the Aptian time.

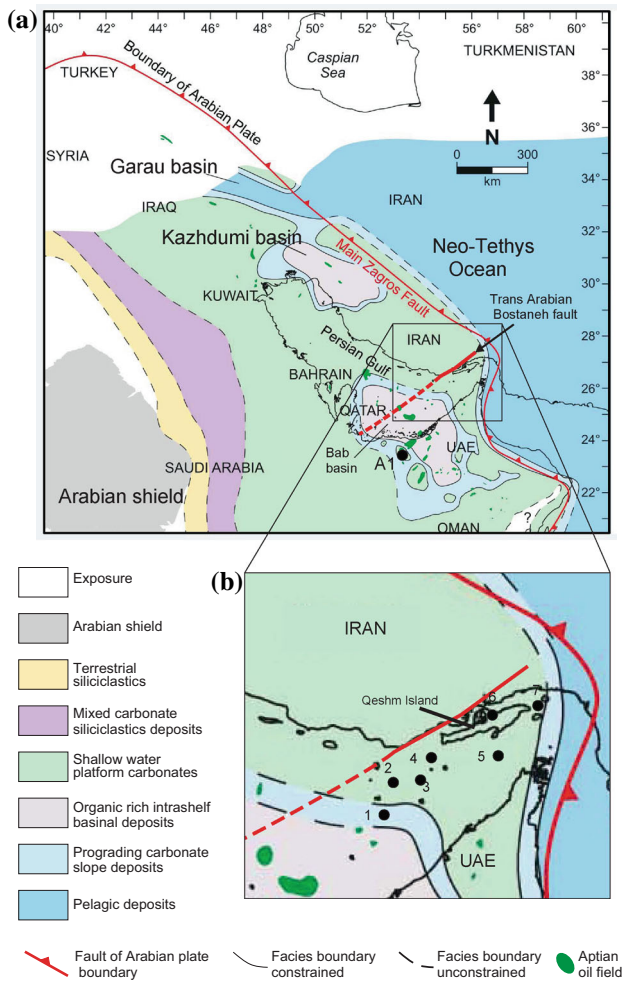

Fig. 2 **a** Early Aptian paleogeographic map of the eastern Arabian Plate (from Van Buchem et al. 2010a) with locations of the Persian Gulf, Trans-Arabian Bostaneh basement fault (Bahroudi and Koyi 2004) and studied area, A1: location of one of Abu Dhabi's fields containing wells which were used in Fig. 10; **b** location of studied wells (1–7)

2 Geological setting

The Persian Gulf Basin (Fig. 2) developed in the offshore part of Zagros Belt in the northeast of the Arabian Plate (Edgell 1996; Alavi 2004). This basin is situated in the Arabian Peninsula (Konyuhov and Maleki 2006) and its eastern part is called the Shilaif Basin or the northern part of Rub al-Khali and Ras al-Khaimah subbasins (Alsharhan and Nairn 1997). The Persian Gulf and Zagros Mountains have a similar sedimentary record encompassing strata ranging in age from the latest Precambrian to the Recent (James and Wynd 1965; Berberian and King 1981; Motiei 1993; Alavi 2004). The total thickness of these successions from the deformed Fars region in the north to the nearly undeformed strata of Persian Gulf region reaches about 7 km (Alavi 2007). Following Neotethys opening in Middle to Late Permian between the Cimmerian continental blocks and the eastern margin of the Arabian Plate (e.g., Bechennec et al. 1990; Ruban et al. 2007), a stable passive carbonate platform (lasting for over 160 Myrs) was established during the Triassic to late Cretaceous (Cenomanian) that simultaneously subsided due to post-rift thermal subsidence (Glennie 2000; Sharland et al. 2001; Piryaei et al. 2011; Ali et al. 2013).

After rising sea level during Early Cretaceous time, the upper part of the Khami Group sediments (Fahliyan, Gadvan, and Dariyan Formations) were deposited on a gently eastward dipping carbonate ramp over Jurassic evaporites (Hith Formation) (Alsharhan and Nairn 1997) and exhibit significant variation in thicknesses. During the onset of Neotethys subduction in the Aptian (Glennie 2000), the Dariyan Formation has been deposited in a carbonate platform to intrashelf basin in the northeastern passive margin of the Arabian Plate (Schroeder et al. 2010; Van Buchem et al. 2010b; Vincent et al. 2010) that was followed by deposition of Burgan sandstone equivalent sediments of latest Aptian to Early Albian age. This formation is equivalent to the Shu'aiba Formation and Hawar Member (Aptian carbonate sediments) of the Arabian Plate and deepened toward the Kazhdumi intrashelf basin in southwest Iran and the Bab intrashelf basin in UAE containing high levels of organic matter (Schroeder et al. 2010; Van Buchem et al. 2010b) (Figs. 1, 2). The Burgan sandstone deposited during a long break in the carbonate sedimentation in the Fars area (adjacent to the studied area) and other parts of the Arabian Plate (Van Buchem et al. 2010a, b).

At the other side, halokinetic tectonism produced by salt movements of Late Pre Cambrian-Early Cambrian age Hormuz and equivalent series has further effects on this region (Ala 1974; Sadooni 1993; Motiei 2001; Jahani et al. 2007). Salt movements have considerable effects on facies changes and shallowing or deepening of Cretaceous sedimentary basins in the studied region (e.g., Piryaei et al. 2011).

3 Study methods

Detailed paleontological, sedimentological, and well log analysis were performed on 7 wells throughout Qeshm Island and offshore area (Fig. 2) and correlated with other studies of the Dariyan Formation in this region. These wells are from a large area across the eastern part of the Persian Gulf and the thickness of the Dariyan Formation ranges from 70 to 122 m. Three hundred core and cutting thin sections were studied by petrographic microscopy to determine the lithofacies and fossil components. Carbonate rocks were classified according to the Dunham (1962), and Embry and Klovan (1971) schemes. Lateral and vertical lithofacies changes were determined using well logs, cores, and cutting data, and depositional environments were interpreted using methods such as those presented by Flugel (2010). Along with biostratigraphic and lithofacies studies, gamma ray and acoustic well logs have an important role for stratigraphic correlation in the Dariyan. Similar to regions to the south such as Oman and UAE (e.g., Vahrenkamp 2010; Droste 2010), the gamma log profile has a similar shape over most of studied area. This profile starts with a high gamma spike at the base of the Hawar Member followed by a sharply decreasing trend, and a more or less constant slightly increasing trend upward. With regard to a lower amount of argillaceous material in the lower parts of the Dariyan Formation, gamma ray logs over the Lower Shu'aiba can reflect variations of uranium content of organic materials under reducing conditions (e.g., Wignall and Myers 1988). On the other hand, the high gamma ray content in the Hawar and top of the Dariyan Formation probably is due to propagation of exposure surfaces and may have been related to concentration by groundwater movement (Ehrenberg and Svånå 2001; Droste 2010). In all wells, the boundary between the Burgan and Dariyan Formations was characterized by a high gamma spike and high acoustic response due to clastic influx during deposition of these formations. Applying essential concepts to determine sequence boundaries and comparing gamma ray and sonic logs as well as paleolog data with Arabian Plate sequences, we interpret depositional sequences and sea-level changes during deposition of the Dariyan Formation.

4 Biostratigraphy

Schroeder et al. (2010) produced a chronostratigraphic correlation of Oman, UAE, and southwest Iran according to Orbitolinids (Fig. 1) that helps us in correlating stratigraphic units of the Persian Gulf. According to this correlation, the Early to Late Aptian Dariyan Formation is equivalent to both the Hawar Member and Shu'aiba Formation, and the Barremian Gadvan Formation correlates with the Kharaib Formation. In this study, we used all paleolog data (Jalali 1969; Nayebi 2000, 2001; Azimi 2010a, b; Hadavandkhani 2010; Fonooni 2010) and revised orbitolinid biostratigraphic zonation for the Barremian–Aptian of the eastern Arabian Plate (Schroeder et al. 2010) to identify biozones in studied wells. In paleologs, the Dariyan and Gadvan Formations with *Choffatella decipiens* and *Palorbitolina lenticularis* (Late Barremian to the Early/Late Aptian age) show the *Palorbitolina lenticularis* biozone and intervals containing *Dictyoconus arabicus* (*Montseciella arabica*) can be differentiated as a *Montseciella arabica* subzone. This subzone in eastern Arabian and northeastern African plates appeared approximately from the middle to end of the Late Barremian time. In this study, similar to southwest Iran (Van Buchem et al. 2010b), this subzone exists in the Barremian age Gadvan Formation (Kharaib equivalent). In paleolog of well 1, Early Late Aptian age can be related to the time range from appearance of *Mesorbitolina parva* to *Mesorbitolina texana*. Occurrence of *Mesorbitolina texana* coincides with a late Late Aptian age for the upper part of the Dariyan Formation in this well. The presence of *Hemicyclammina sigali* of Albian age in Kazhdumi and Burgan sandstones in studied wells is a key to separating the Aptian–Albian boundary as mentioned by Schroeder et al. (2010).

5 Lithofacies analysis

14 carbonate lithofacies (Figs. 3, 4; Table 1), which were grouped into three lithofacies associations, were identified in the Dariyan Formation similar to the Shu'aiba and Hawar Formations in Arabian parts (e.g., Raven et al. 2010; Van Buchem et al. 2010a, b). These were deposited in a carbonate ramp system to intrashelf basin (Fig. 5) as follows:

5.1 Shallow inner ramp lithofacies association

This lithofacies association consists of sandy mudstone, milliolidae wackestone/pellet grainstone, benthic foraminifera wackestone/pellet grainstone, and conical Orbitolina wackestone/packstone (Fig. 3; Table 1). This lithofacies mainly deposited during deposition of the lower part of the Dariyan Formation on a shallow carbonate ramp. The abundance of mud-dominated textures, existing milliolidae benthic foraminifers, the low abundance, and diversity of open marine fauna/flora are consistent with deposition within a restricted, shallow-water, low-energy lagoonal setting (Flugel 2010; Pittet et al. 2002). The milliolids are intolerant to oxygen-deficient conditions and increase in abundance according to food availability, when oxygen is not a limiting factor (Halfar and Ingle 2003). In grainstone lithofacies, shallow marine higher energy

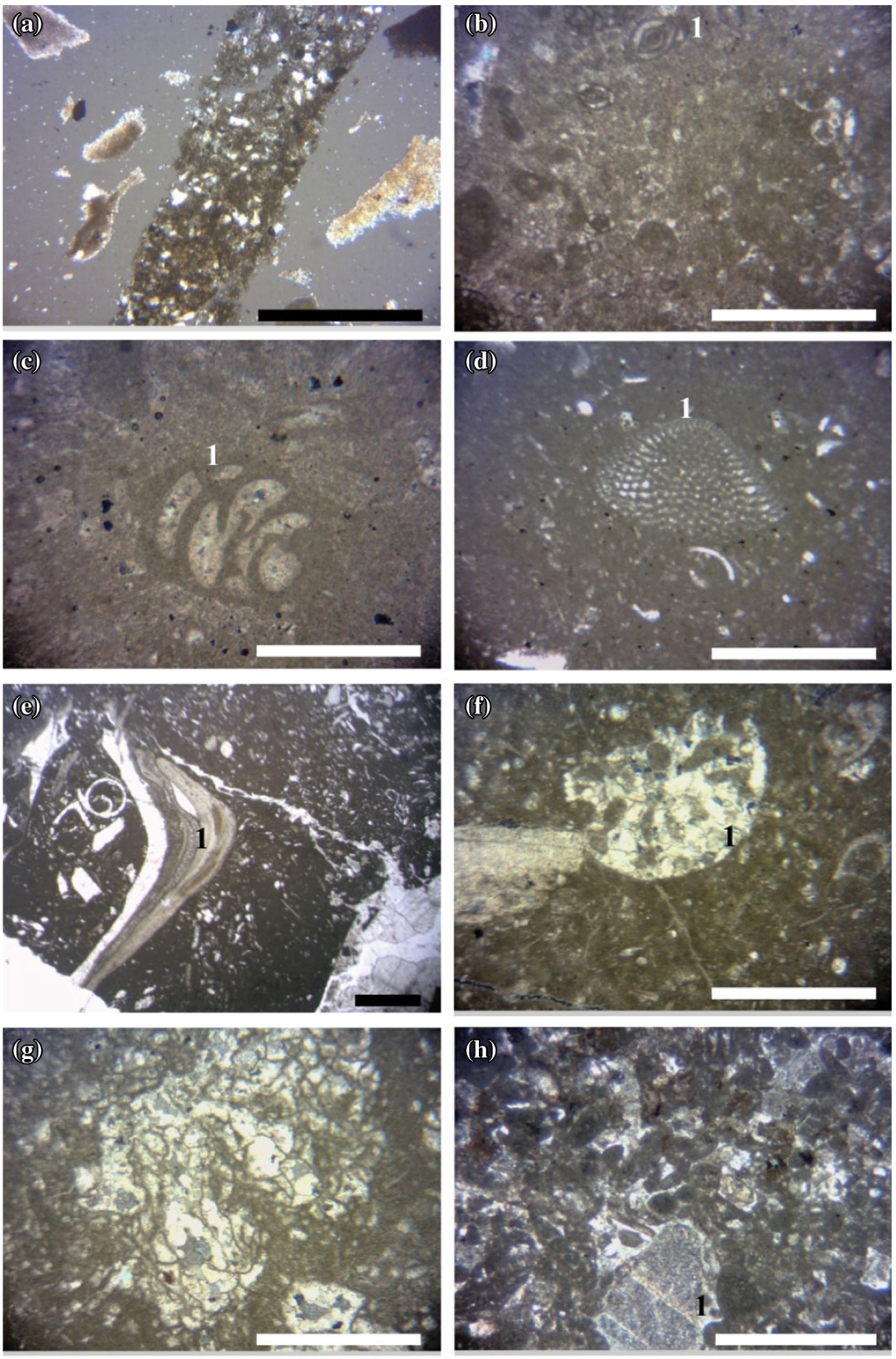

Fig. 3 Dariyan Formation lithofacies in studied wells, **a** sandy mudstone (A1), well 5, depth: 4257 m, PPL; **b** milliolidae wackestone/pellet grainstone (A2), *1* Milliolidae, well 1, 9758 ft, XPL; **c** Benthic foraminifera wackestone/pellet grainstone (A3), *1* Dukhania, well 1, 9747 ft, XPL; **d** conical Orbitolina wackestone/packstone (A4), *1* Conical Orbitolina, well 1, 9645 ft, XPL; **e** rudist rudstone (B1), *1* Rudist debris, well 1, 9711 ft, PPL; **f** coral rudstone (B2), *1* coral fragment, well 1, 9743 ft, XPL; **g** *Lithocodium aggregatum* rudstone/boundstone (B3), well 1, 9750 ft, XPL; **h** echinoid pellet grainstone (B4), *1* Echinoid debris, well 2, 10,890 ft, XPL. Scale bar = 1 mm

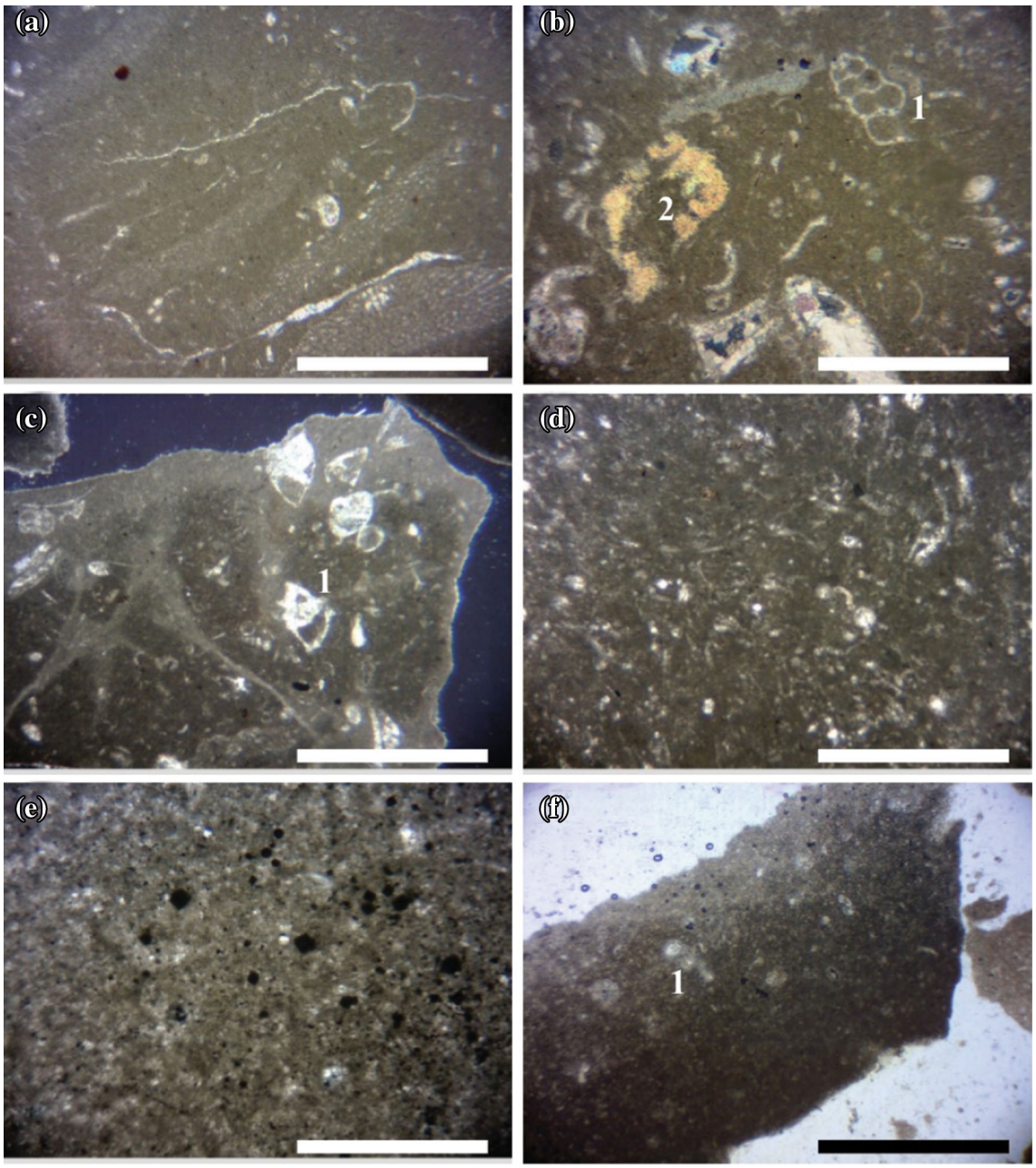

Fig. 4 Dariyan Formation lithofacies in studied wells, **a** discoidal Orbitolina wackestone/packstone, well 1, 9698 ft, XPL; **b** bioclastic wackestone/packstone (B5), well 1, *1* Gastropod, *2* Echinoid, 9692 ft, XPL; **c** lenticulina/epistomina wackestone (C1), well 6, *1* lenticulina, 9950-55 ft, XPL; **d** sponge spicule wackestone/packstone (C2), well 2, 10,730 ft, PPL; **e** pyritized mudstone (C4), well 1, 9633 ft, PPL; **f** Pelagic foraminifera wackestone (C3), well 6, *1* Globigerina, 9885-90 ft, PPL. Scale bar = 1 mm

conditions created grainstone textures in bars and local platform topographic highs. Conical Orbitolina packstone/wackestone consists mainly of conical forms of orbitolinids that are related to shallower water environmental settings (e.g., Vilas et al. 1995; Simmons et al. 2000; Hughes 2000; for further details see Pittet et al. 2002). Benthic foraminifers such as trocholina indicate lagoonal and shallow marine lithofacies (e.g., Meyer 2000; Hughes 2004, 2005). Dasyclad green algae such as salpingoporella dinarica are other common constituents of this lithofacies association that proves a restricted lagoon environment.

5.2 Mid-ramp lithofacies association

This lithofacies association contains rudist rudstone, coral rudstone, lithocodium aggregatum rudstone/boundstone,

Table 1 Lithofacies analysis of Dariyan Formation

Lithofacies association	Lithofacies	Texture	Major components	Minor components	Depositional environment
A	A1	Sandy mudstone	Terrigenous material, pellet	Trocholina, pyrite, milliolidae	Inner ramp-tidal flat
	A2	Milliolidae wackestone/pellet grainstone	Milliolidae, nezzazata, pellet, intraclast, dasyclad green algae, bivalve, pellet	Trocholina, Orbitolina, textularia, acicularia, dukhania	Inner ramp-restricted lagoon and bar
	A3	Benthic foraminifera wackestone/pellet grainstone	Dukhania, trocholina, milliolidae, nezzazata, pellet, intraclast	Orbitolina, textularia, pyrite, acicularia, gastropod, dasyclad green algae	Inner ramp-restricted lagoon and bar
	A4	Conical Orbitolina wackestone/packstone	Conical Orbitolina, textularia, dukhania, pellet	Echinoid, dasyclad green algae, discoidal Orbitolina, terrigenous material, pyrite, gastropod, rudist debris	Inner ramp-restricted to open lagoon
B	B1	Rudist rudstone	Rudist, lithocodium aggregatum, gastropod, bivalve	Echinoid, conical and discoidal Orbitolina, coral, dasyclad green algae, textularia, pellet	Mid-ramp
	B2	Coral rudstone	Coral, rudist, Orbitolina	Lithocodium aggregatum, benthic foraminifera, dasyclad green algae, pellet	
	B3	Lithocodium aggregatum rudstone/boundstone	Lithocodium aggregatum, rudist, Orbitolina, coral, spongiomorphid, bivalve	Benthic foraminifera, dasyclad green algae, pellet	
	B4	Echinoid pellet grainstone	Echinoid, pellet, discoidal Orbitolina, bivalve, lithocodium aggregatum	Oyster, gastropod, salpingoporella dinarica	
	B5	Discoidal orbitolina wackestone/packstone	Discoidal Orbitolina	Choffatella decipiens, rudist, echinoid, gastropod, conical Orbitolina, bivalve, benthic and pelagic foraminifera, sponge spicule, terrigenous material	
	B6	Bioclastic wackestone/packstone	Echinoid, bivalve, gastropod	Pelagic foraminifera, sponge spicule, oyster, pellet, discoidal Orbitolina, lenticulina	
C	C1	Lenticulina/epistomina wackestone	Lenticulina, epistomina	Pelagic foraminifera, sponge spicule, choffatella decipiens, bivalve, Orbitolina	Outer ramp
	C2	Sponge spicule wackestone/packstone	Sponge spicule, echinoid, lenticulina, calcispher	Echinoid, debarina, pelagic foraminifera, Orbitolina, radiolaria	Outer ramp-intrashelf
	C3	Pyritized mudstone	Pyrite, terrigenous material, calcispher, pellet	Radiolaria, Orbitolina	Intrashelf
	C4	Pelagic foraminifera wackestone	Globigerina, radiolaria	Sponge spicule, radiolaria, pellet	Intrashelf

echinoid pellet grainstone, discoidal Orbitolina wackestone/packstone, and bioclastic wackestone/packstone (Figs. 3, 4; Table 1). This lithofacies association is characterized by a higher content of open marine bioclasts and existing large rudist shells, corals, and lithocodium aggregatum faunas. Rudist rudstone and lithocodium aggregatum rudstone/boundstone are typical lithofacies of the Dariyan Formation and have been studied and reported from the Shu'aiba Formation in nearby regions (e.g., Van Buchem et al. 2002; Maurer et al. 2010; Pierson et al. 2010). In the studied wells, these two lithofacies sometimes coexisted with each other indicating deposition in similar conditions. Rudists have developed in greater abundance on the southern part of the Arabian Plate (UAE: Wilson 1975; Yose et al. 2006; Oman: Witt and Gökdag 1994; Masse et al. 1997; Van Buchem et al. 2002; Boote and Mou 2003; Qatar: Raven et al. 2010) than southwest Iran (Van Buchem et al. 2010b) and form the main reservoirs in that area (e.g., Amthor et al. 2010). This lithofacies is mainly found in upper parts of the Dariyan Formation and the similar Shu'aiba Formation (e.g.,

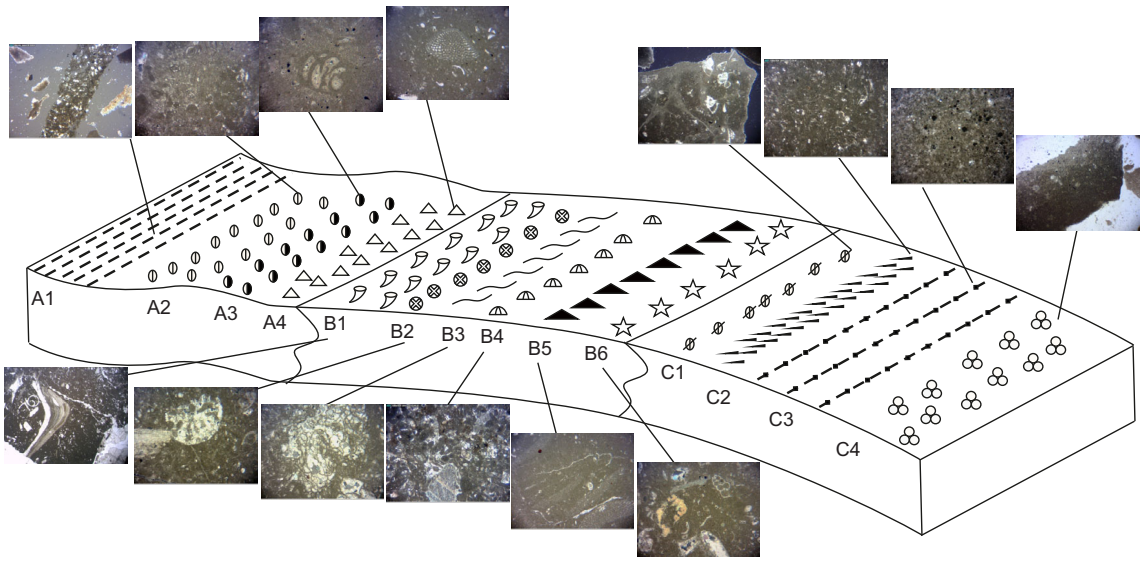

Fig. 5 Depositional model for carbonate sediments of the Dariyan Formation

Vahrenkamp 2010; Yose et al. 2010). It may be formed as a bank and build-ups in the shallow marginal parts of Aptian carbonate platforms with diverse faunas. On the other hand, coral rudstone/boundstone, which sometimes coexists with lithocodium aggregatum rudstone/boundstone and rudist rudstone is another mid-ramp environment lithofacies. Similar to nearby regions (e.g., Granier et al. 2003; Van Buchem et al. 2010a, b), lithocodium aggregatum rudstone/boundstone deposited during the initial construction phase of the Shu'aiba platform and rudists nucleated on them. Lithocodium aggregatum is a very common association in the Early Aptian (Immenhauser et al. 2004, 2005; Hillgärtner et al. 2003) and has a paleogeographic range that is comparable to tropical and subtropical reefs in the Mesozoic (Rameil et al. 2010). This lithofacies quickly colonized and started aggrading following the rise of sea level in the fair-weather wave base area in the shelf margin near rudist rudstones (e.g., Hillgärtner 2010). Echinoid pellet grainstone lithofacies mainly contains open marine echinoid bioclasts and deposited in high-energy conditions of platform margin bars and pellet grains probably transported from shallower areas such as lagoons. The discoidal Orbitolina packstone/wackestone consists mainly of discoidal forms of orbitolinids that are formed in deeper parts of open marine environments in platform margin conditions and probably were deeper than units with abundant lithocodium aggregatum. The flattened form of palorbitolina is probably a response to the relatively low-light setting, therefore indicating their formation in deeper parts of mid-ramp (Immenhauser et al. 1999; Simmons et al. 2000). Finally, bioclastic wackestone/packstone lithofacies consist mainly of diverse bioclasts and were deposited in a low-energy shelf margin to slope conditions.

5.3 Outer ramp/intrashelf basin lithofacies association

This association deposited on the outer ramp or after creation of the intrashelf basin. It consists of lenticulina/epistomina wackestone, sponge spicule wackestone/packstone, pyritized mudstone, and pelagic foraminifera wackestone lithofacies (Fig. 4; Table 1). Sponge spicule wackestone consists mainly of deeper water sponge spicules (Flugel 2010), which were deposited in the outer ramp to intrashelf basin. The occurrence of lenticulina and epistomina along with some pelagic foraminifera in lenticulina/epistomina wackestone also prove deeper marine conditions (Meyer 2000). Pyritized mudstone is another lithofacies that deposited in reducing conditions. Some deep-sea faunas such as radiolaria, sponge spicule, and pelagic foraminifers were identified in this lithofacies and other lithofacies of this association. Pelagic foraminifera wackestone lithofacies is another deep-water lithofacies that contains diverse globigerina and hedbergella faunas within a dark micritic context that partly has been pyritized in reducing conditions.

6 Sequence stratigraphy

Sequence stratigraphy of the Barremian–Aptian strata in the Arabian Plate has been studied in outcrop (Pittet et al. 2002; Van Buchem et al. 2002, 2010b) and subsurface (Sharland et al. 2001; Yose et al. 2010; Maurer et al. 2010; Pierson et al. 2010). The Dariyan Formation (equivalent to the Shu'aiba Formation and Hawar Member) deposited during Aptian supersequence transgressive–regressive cycles and was bounded by unconformities (Yose et al.

2010). Van Buchem et al. (2010a) also proposed a new sequence stratigraphic framework that correlates through the Arabian Plate and Persian Gulf region of this plate. According to this framework, the Arabian Plate Aptian Supersequence was divided into four third-order sequences, named Arabian Plate Aptian Sequences 1 to 4 (abbreviated: Apt 1–Apt 4; Table 2). The Apt 5 third-order sequence of the Late Aptian–Albian supersequence is another sequence that was identified in carbonate sequences of the Dariyan Formation (Van Buchem et al. 2010a; Table 2). Identification of these sequences in the studied area is according to correlation of log data and lithofacies characteristics with Arabian Plate sequences. Table 2 shows some characteristics of these sequences in the Arabian Plate and the studied area, and Fig. 13 shows the correlation of these sequences with each other and Arabian Plate Apt 1–5 sequences in Abu Dhabi. Time ranges of each third-order sequence are according to GTS time scale of Ogg et al. (2004).

6.1 Apt 1 sequence (from 125 to 124.6 Ma)

This sequence comprises the Lower Dariyan Formation (equivalent to the lower Shu'aiba Formation and Hawar Member). The base of this sequence in the Arabian platform shows evidence of exposure and is the lower boundary of a second-order sequence (Vahrenkamp 2010; Van Buchem et al. 2010b) with an abrupt gamma ray increases probably due to uranium concentration by groundwater movement. In offshore Abu Dhabi, Granier (2008) interpreted the Hawar Member as an unconformity-bounded unit and Yose et al. (2010) divided this sequence as Apt 1a (Hawar Member) and Apt 1b (Lower Shu'aiba). According to chronostratigraphic studies of Schroeder et al. (2010) (Fig. 1), there was a hiatus between the Hawar Member and Kharaib Formation (equivalent to the Gadvan Formation) so we can interpret this boundary as a type 1 sequence boundary. In the studied wells, the trend in gamma ray readings is similar to other parts of the Arabian platform and the lower boundary of the Dariyan Formation is thought to be an exposure surface. This sequence consists of shallow inner to mid-ramp lithofacies with similar thicknesses ranging from 12 to 23 m. This sequence in the Arabian platform forms an intraformational seal or dense unit (Van Buchem et al. 2002). This sequence formed TST and HST that are described below:

6.1.1 TST

Transgressive system tract (TST) lithofacies mainly consists of sandy mudstone, milliolidae wackestone/pellet grainstone, benthic foraminifera wackestone/pellet grainstone, echinoid pellet grainstone, discoidal Orbitolina wackestone, and bioclastic wackestone/packstone. Thickness of TST lithofacies ranges from 4 m to 13 m and the shallowest sandy mudstone lithofacies was identified in

Table 2 Characteristics of Arabian Plate Aptian sequences (Van Buchem et al. 2010a) and the studied area

Super sequences	Third-order sequences/age	Characteristics in the Arabian Plate	This study (main characteristics)
Late Aptian–Albian	Apt 5 (LST)/Late Aptian	Deposition of mixed argillaceous/carbonate sediments on exposed sequence boundary	In well 1: TST: B5 HST: A4
Aptian	Apt 4 (Late HST)/latest Early Aptian to early Late Aptian	Progradation of slope-restricted fringing shoals and carbonate mud banks in low-angle clinoforms, development of small rudist shoals and orbitolinid-dominated slopes	In wells 1, 5, and 6: TST: A4, B2, B5, B6, C3, C4 HST: B1, B2, C1, C2, C3, C4
	Apt 3 (Early HST)/latest Early Aptian	Rudist-dominated platform aggradation and progradation, basin starvation, production surpasses accommodation space.	TST: A2, A3, A4, B1, B3, B4, B5, B6, C1, C2, C4 HST: A1, A2, A3, A4, B1, B3, B5, C1, C2, C4
	Apt 2 (Late TST)/late Early Aptian	Development of topographic relief, proliferation of lithocodium–bacinella boundstone lithofacies, which formed mound-like features and eventually aggradational platforms, the time-equivalent starvation of the intrashelf basins where a condensed organic-rich sedimentation took place, time-equivalent to the OAE-1a event	TST: A2, A3, B2, B3, B5, B6, C3, C4 lithofacies HST: A1, A3, B5, B6, C1, C3, C4 lithofacies
	Apt 1 (Early TST)/early Early Aptian	Development of flat, orbitolinid-dominated, argillaceous low-angle ramp system, known as the Hawar member	TST & HST: A1, A2, A3, B4, B5, and B6 lithofacies

wells 5 and 7. The maximum flooding surface lies in low gamma ray lithofacies such as echinoid pellet grainstone, bioclastic wackestone/packstone, and discoidal Orbitolina wackestone/packstone (Figs. 6, 7, 8, 9, 10, 11, 12).

6.1.2 HST

The thickness of highstand system tract (HST) lithofacies ranges between 2 and 10 m and shallowest inner ramp sandy mudstone lithofacies deposited in wells 5 and 7. The upper boundary of this sequence is type 2 and is positioned at the top of sandy mudstone, milliolidae wackestone/pellet grainstone, benthic foraminifera wackestone/pellet grainstone, discoidal Orbitolina wackestone, and bioclastic wackestone/packstone lithofacies (Figs. 6, 7, 8, 9, 10, 11, 12).

6.2 Apt 2 sequence (from 124.6 to 124 Ma)

Apt 2 is an age equivalent to the global oceanic anoxic event (OAE1a) (Van Buchem, 2010a; Yose et al. 2010). This sequence is bounded by type 2 sequence boundaries and is indicated by development of lithocodium boundstone lithofacies along with other inner to outer ramp lithofacies. In wells 1, 2, 5–7, the upper part of this sequence shows higher gamma spikes than lower parts. In the lower Shu'aiba Formation, this trend reflects variations in reducing conditions/organic matter content rather than clay content (Droste 2010). Similar to other studies (e.g., Vahrenkamp 2010), the maximum flooding surface is placed near a high gamma ray spike and represents the maximum flooding surface of the Aptian supersequence. In studied wells, this sequence thickened in well 2 (29 m) and thinned toward wells 6 (12 m) and 1 (15 m). This sequence consists of TST and HST as follows:

6.2.1 TST

The thickness of TST lithofacies ranges between 6 and 24 m and mainly starts with developing lithocodium boundstone lithofacies. Other lithofacies consists of milliolidae wackestone/pellet grainstone, benthic foraminifera wackestone/pellet grainstone, coral rudstone, discoidal Orbitolina wackestone/packstone, bioclastic wackestone/packstone, lenticulina/epistomina wackestone, pyritized mudstone, and pelagic foraminifera wackestone. The deepest lithofacies (pyritized mudstone and pelagic foraminifera wackestone) is identified in wells 5 and 6 and the maximum flooding surface is mainly placed near high spike gamma ray readings (Figs. 6, 7, 8, 9, 10, 11, 12).

6.2.2 HST

Lithofacies of HST consist of sandy mudstone, benthic foraminifera wackestone/pellet grainstone, discoidal Orbitolina wackestone/packstone, bioclastic wackestone/packstone, lenticulina/epistomina wackestone, pyritized mudstone, and pelagic foraminifera wackestone (Figs. 6, 7, 8, 9, 10, 11, 12). The thickness of HST facies changes from 1 to 13 m and the upper part of this sequence is bounded by a type 2 sequence boundary. During deposition of HST, the shallowest lithofacies deposited in well 5 (sandy mudstone) which is probably related to reactivation of older faults.

6.3 Apt 3 (from 124 to 121 Ma)

During this stage, the lithocodium boundstone facies was replaced by colonized rudist and probably formed build-up and flank complexes. According to Al-Husseini and Matthews (2010), Apt 2 and Apt 3 represent the differentiation of the southeastern Arabian Plate into the Shu'aiba Platform and intrashelf Bab Basin. In studied wells, this sequence has a type 2 lower boundary and the upper boundary with the Burgan Formation in wells 2, 3, 4, and 7 is type 1. The thickness of this sequence ranges from 11 to 86 m. This sequence thickened toward well 3 (86 m) and thinned toward SW in wells 1 and 2 and NE in wells 4, 5, and 6. Higher thickness of carbonates in wells 2, 3, 4, and 7 represents good carbonate productivity during platform shallowing and deposition of mid-ramp build-ups toward the location of these wells (Figs. 6, 7, 8, 9, 10, 11, 12). This sequence also consists of TST and HST as follows:

6.3.1 TST

The thickness of TST facies ranges from 7 to 39 m and consists of milliolidae wackestone/pellet grainstone, benthic foraminifera wackestone/pellet grainstone, conical Orbitolina wackestone/packstone, rudist rudstone, lithocodium aggregatum rudstone/boundstone, echinoid pellet grainstone, discoidal Orbitolina wackestone/packstone, bioclastic wackestone/packstone, lenticulina/epistomina wackestone, sponge spicule wackestone/packstone, and pelagic foraminifera wackestone. In wells 1, 5, and 6, the maximum flooding surface is placed at a high gamma ray spike containing discoidal Orbitolina wackestone/packstone, lenticulina/epistomina wackestone, and pelagic foraminifera wackestone lithofacies (Figs. 6, 7, 8, 9, 10, 11, 12).

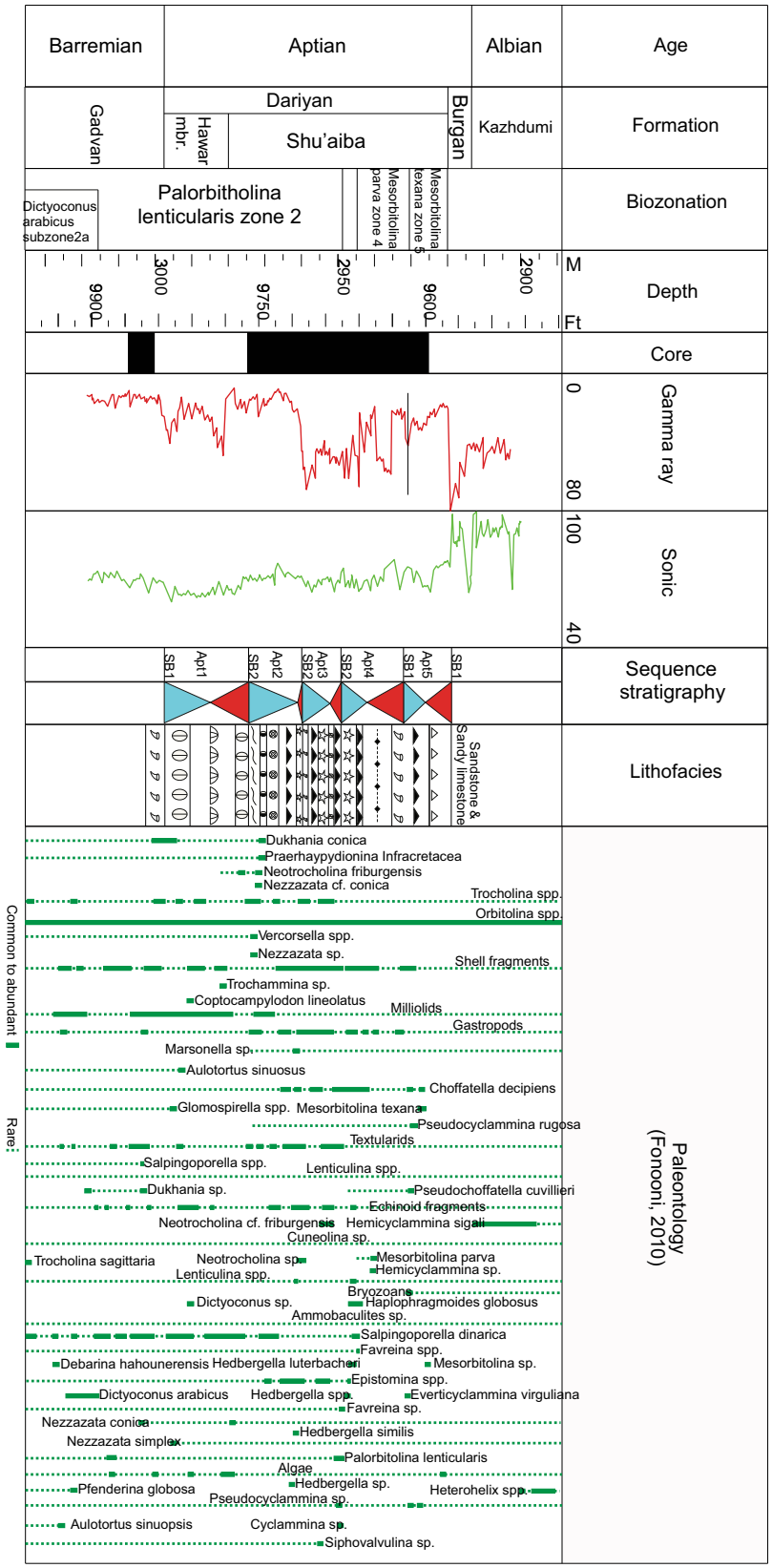

Fig. 6 Sequence stratigraphy, paleontology, gamma ray, and sonic logs in well 1, for lithofacies symbols see Fig. 5

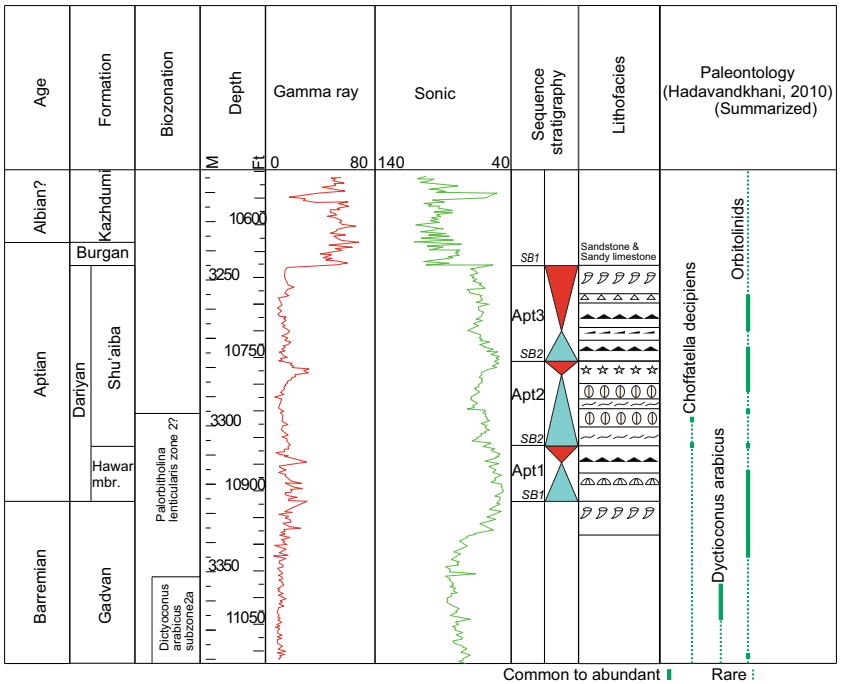

Fig. 7 Sequence stratigraphy, paleontology, gamma ray, and sonic logs in well 2, for lithofacies symbols see Fig. 5

6.3.2 HST

The thickness of HST facies ranges from 3 to 51 m. This phase contains sandy mudstone, milliolidae wackestone/pellet grainstone, benthic foraminifera wackestone/pellet grainstone, conical Orbitolina wackestone/packstone, rudist rudstone, lithocodium aggregatum rudstone/boundstone, discoidal Orbitolina wackestone/packstone, lenticulina/epistomina wackestone, sponge spicule wackestone/packstone, and pelagic foraminifera wackestone. During this phase of deposition, the shallowest sandy mudstone lithofacies were deposited in well 4. The upper boundary is type 2 in wells 1, 5, and 6, and type 1 in wells 2–4 and 7.

6.4 Apt 4 (from 121 to 117.9 Ma)

During this stage, sea level dropped in the Arabian Plate so most parts of the Shu'aiba Platform were exposed and sediments only deposited along the Bab Basin (Al-Husseini and Matthews 2010). Similarly, studied wells 2, 3, 4, and 7 were exposed and Apt 4 did not develop in these wells while deposition continued in wells 1, 5, and 6. Therefore, the lower boundary of Apt 4 in these wells is type 2 and the upper boundary with LST Apt 5 sequence is type 1. Biozonation of well 1 confirms an Early Late Aptian age for Apt 4. Note, in wells 5 and 6, the time range of Apt 4 could not be identified because of the absence of index fossils (Figs. 6, 10, 11). In well 1 (Fig. 6), the thickness of this sequence is about 17 m and contains Mesorbitolina parva with discoidal Orbitolina wackestone/packstone, bioclastic wackestone/packstone, pyritized mudstone, and rudist rudstone lithofacies. The maximum flooding surface is placed at the high gamma ray pyritized mudstone lithofacies. In well 5 (Fig. 10), the thickness of this sequence is about 30 m and contains coral rudstone, conical Orbitolina wackestone/packstone, and pyritized mudstone, and the maximum flooding surface is placed in this well at high gamma ray pyritized mudstone lithofacies. In well 6 (Fig. 11), the thickness of this sequence reaches 30 m and contains pelagic foraminifera wackestone, sponge spicule wackestone/packstone, lenticulina epistomina wackestone, and coral rudstone, and the maximum flooding surface is placed at high gamma ray pelagic foraminifera wackestone.

6.5 Apt 5 (from 117.9 to 112.4 Ma)

This sequence is the lowstand system tract (LST) of the Upper Aptian–Lower Albian Supersequence and deposited during Late Aptian time in mixed argillaceous/carbonate platform. This sequence is depicted in well 1 (Fig. 6) with 13-m thickness and index fossils of Mesorbitolina texana. This sequence consists of conical and discoidal Orbitolina wackestone/packstone lithofacies so the maximum flooding surface is placed at the somewhat high gamma ray discoidal Orbitolina wackestone/packstone lithofacies. As this sequence deposited after exposure of the platform in the Arabian Plate, the lower boundary with Apt 4 is interpreted

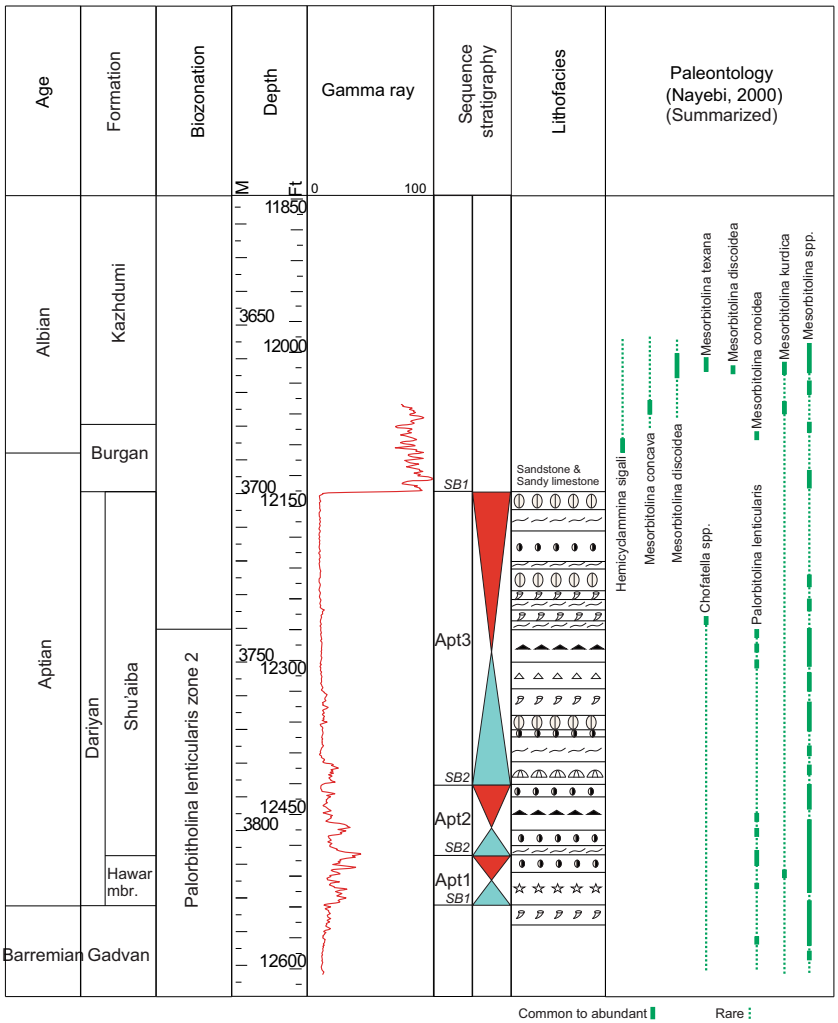

Fig. 8 Sequence stratigraphy, paleontology, and gamma ray log in well 3, for lithofacies symbols see Fig. 5

as type 1 and similarly the upper boundary of this sequence with clastic sediments of the Burgan Formation is also interpreted as a type 1 boundary.

7 Discussion

The sequence stratigraphic correlation of the Dariyan Formation in studied wells and Abu Dhabi wells is illustrated in Fig. 13.

Toward well 1, transition from carbonate platform to intrashelf Bab Basin can be seen, so, well 1 is similar to wells near the intrashelf of the Bab Basin of Vahrenkamp (2010) (wells Y and Z in Fig. 13), while the gamma logs of wells 2–4 are similar to the carbonate platform logs of Vahrenkamp (2010). Toward wells 5 (near Qeshm Island) and 6 (in Qeshm Island), there is a rapid deepening trend into deep-water sediments as seen on the high gamma ray logs; therefore, we believe there might have been an intrashelf basin in this area (Fig. 14). This proposed regional intrashelf basin has not been reported for the Aptian sediments before in the Persian Gulf region and needs more attention. According to Al-Ghamdi and Read (2010), Early Cretaceous intrashelf basins were created because of Neoproterozoic-Early Cambrian Hormuz salt movement that started as early as the Permian time in the Persian Gulf (Motiei 1995). On the other hand, reactivation of Trans-Arabian Bostaneh basement fault (Bahroudi and Koyi 2004) could have played a major role in the creation of this intrashelf basin. According to Glennie (2000), the start of subduction during the Aptian was accompanied by crustal warping of the Arabian continental platform creating erosional highs and intrashelf euxinic basins between them.

Van Buchem et al. (2002) proposed a mechanism for the creation of the Aptian age Bab intrashelf basin. According to Van Buchem et al. (2002), small topographic

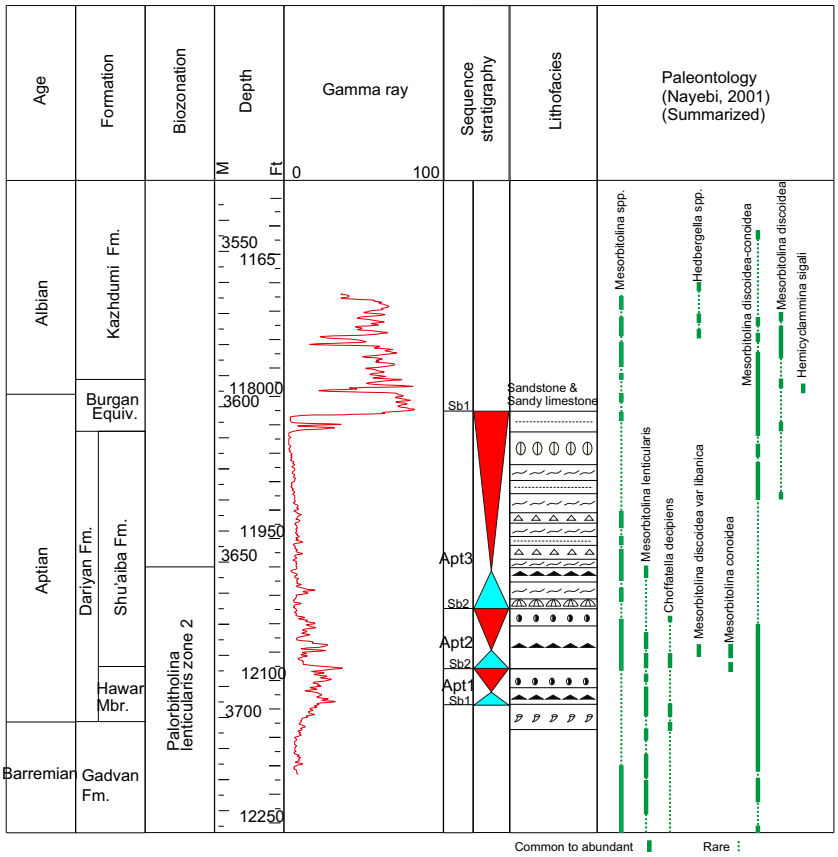

Fig. 9 Sequence stratigraphy, paleontology, and gamma ray log in well 4, for lithofacies symbols see Fig. 5

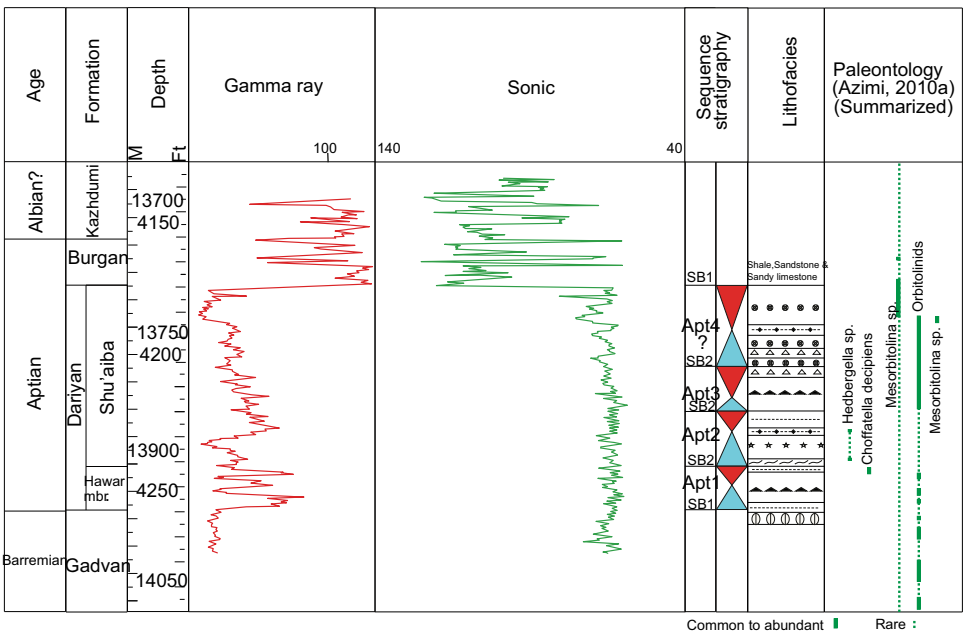

Fig. 10 Sequence stratigraphy, paleontology, gamma ray, and sonic logs in well 5, for lithofacies symbols see Fig. 5

differences are considered to have triggered differential sedimentation rates during an increased rate of relative sea-level rise. We interpret that topographic differences were mainly created by salt movement, crustal warping, and basement fault reactivations (especially the Trans-Arabian Bostaneh fault) in Qeshm Island and adjacent

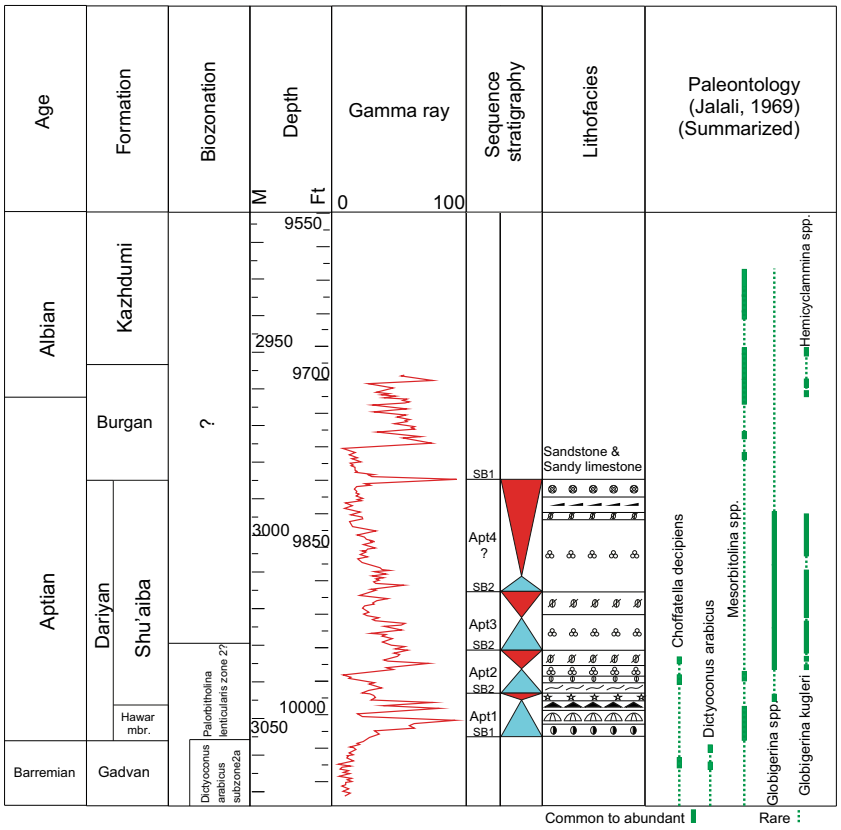

Fig. 11 Sequence stratigraphy, paleontology, and gamma ray log in well 6, for lithofacies symbols see Fig. 5

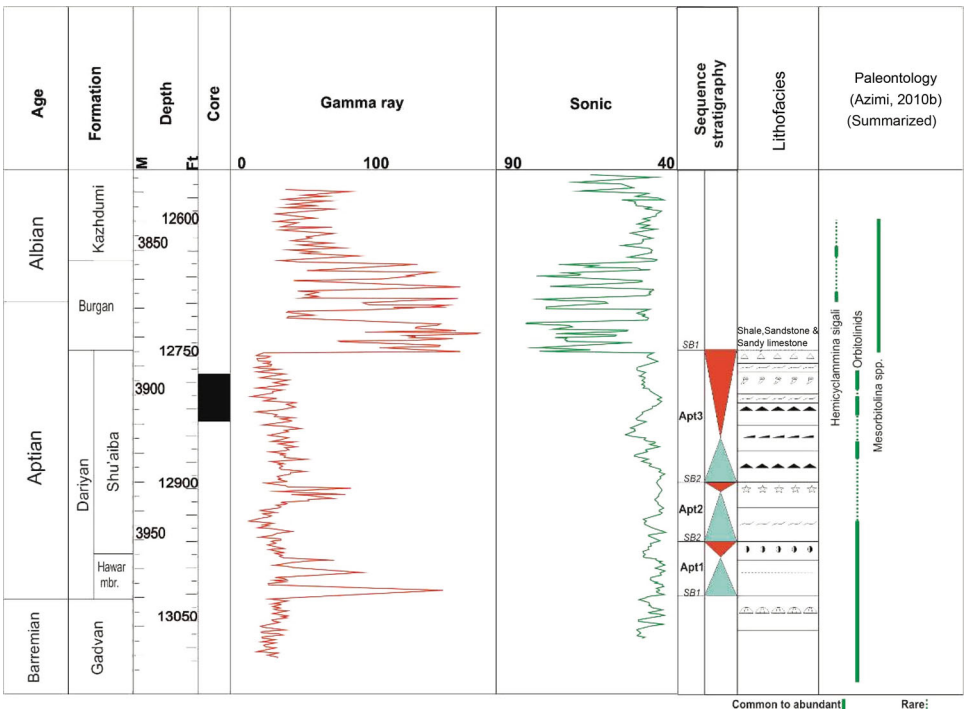

Fig. 12 Sequence stratigraphy, paleontology, gamma ray, and sonic logs in well 7, for lithofacies symbols see Fig. 5

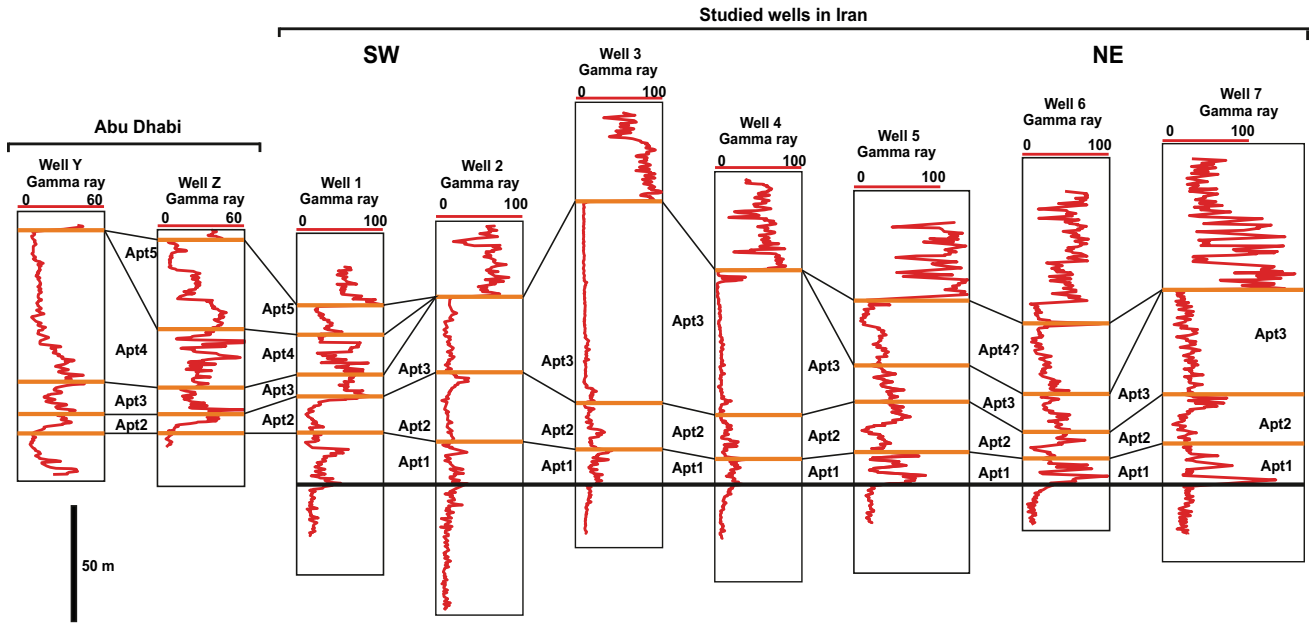

Fig. 13 Sequence stratigraphic correlation between studied wells and comparison of Iranian wells with Abu Dhabi well logs of Vahrenkamp (2010) located in a field near the Bab Basin (Fig. 2)

area. The intrashelf basin, due to conditions such as a stratified water column and slow water circulation, was suitable for the deposition of organic-rich source rock material in the Arabian platform (Van Buchem et al. 2002), so high gamma ray intrashelf deposits in wells 1, 5, and 6 probably have a good source rock capacity. Based on correlation of sequences (Fig. 13) and paleogeographic mapping (Fig. 14), Apt 1 shows similar thicknesses of shallow marine inner to mid-ramp lithofacies. During Apt 1, transgressive onlaps developed toward the eastern exposed area in northern Oman (Droste 2010) (Fig. 14). After the second major transgression (Apt 2), higher differences between sequence thicknesses as well as lithofacies types are due to intrashelf basin topographies. The deepest intrashelf lithofacies of the Apt 2 sequence developed in wells 5 and 6 (Fig. 14). During deposition of Apt 3, the deepest part of the basin is placed in wells 1, 2 (Bab Intrashelf Basin), 6 and 7 (Qeshm Intrashelf Basin) (Fig. 14), while the shallowest part with thickest deposits is located in wells 3–5. Rudist and coral rudstone lithofacies, which probably have good reservoir properties, deposited mid-ramp in wells 2–4, 7, and partly in well 1. After this phase, the Apt 4 sequence developed in wells 1 (Bab Intrashelf Basin), 5, and 6 (Qeshm Intrashelf Basin) (Fig. 14). During this phase, other wells were exposed and Burgan Formation deposited in coastal marine areas (Fig. 14). During the deposition of the Apt 4 interval, rudist and coral rudstone lithofacies deposited in shallow marine environments, probably with good reservoir properties in wells 1, 5, and 6. On the other hand, well 6 contains thicker intrashelf sediments and we interpret that a continuous deepening of the platform existed in well 6. The Apt 5 sequence only developed in well 1 near the Bab Basin and is not present in other wells (Fig. 14). Finally, after deposition of Apt 5, the entire Dariyan carbonate platform was exposed and terrigenous materials of the Burgan Formation deposited after a long break in coastal to shallow marine environment throughout the study area.

Global cooling and warming events (e.g., Herrle and Mutterlose 2003; Mutterlose et al. 2009) played an important role in controlling sea-level changes of the Arabian Plate Cretaceous epicontinental sea and deposition of sequences. The Aptian was a cooler period with some ice sheets at the poles (Al-Ghamdi and Read 2010). According to Van Buchem et al. (2010a), Aptian sedimentation on the Arabian Platform (marginal part of Arabian Plate) was influenced by two cold phases: One short-lived phase in the earliest Aptian and a second longer lived phase in the Late Aptian. These cold phases caused glacio-eustatic large and rapid sea-level fluctuations in the order of 40 m and exposure of the platform before deposition of the Apt 1 and Apt 5 sequences. Extinction of the rudists in Apt 5 of the Arabian Platform and studied area may have been the result of climatic cooling of Aptian seawater (e.g., Strohmenger et al. 2010). Exposure of Aptian sediments in the latest Aptian–Early Albian (upper boundary of Dariyan Formation) also fits with another cooling event that was recognized in sedimentary facies and in the C- and O-isotope records (e.g., Weissert and Lini 1991) and discussed by Raven et al. (2010) in Aptian sediments of Qatar.

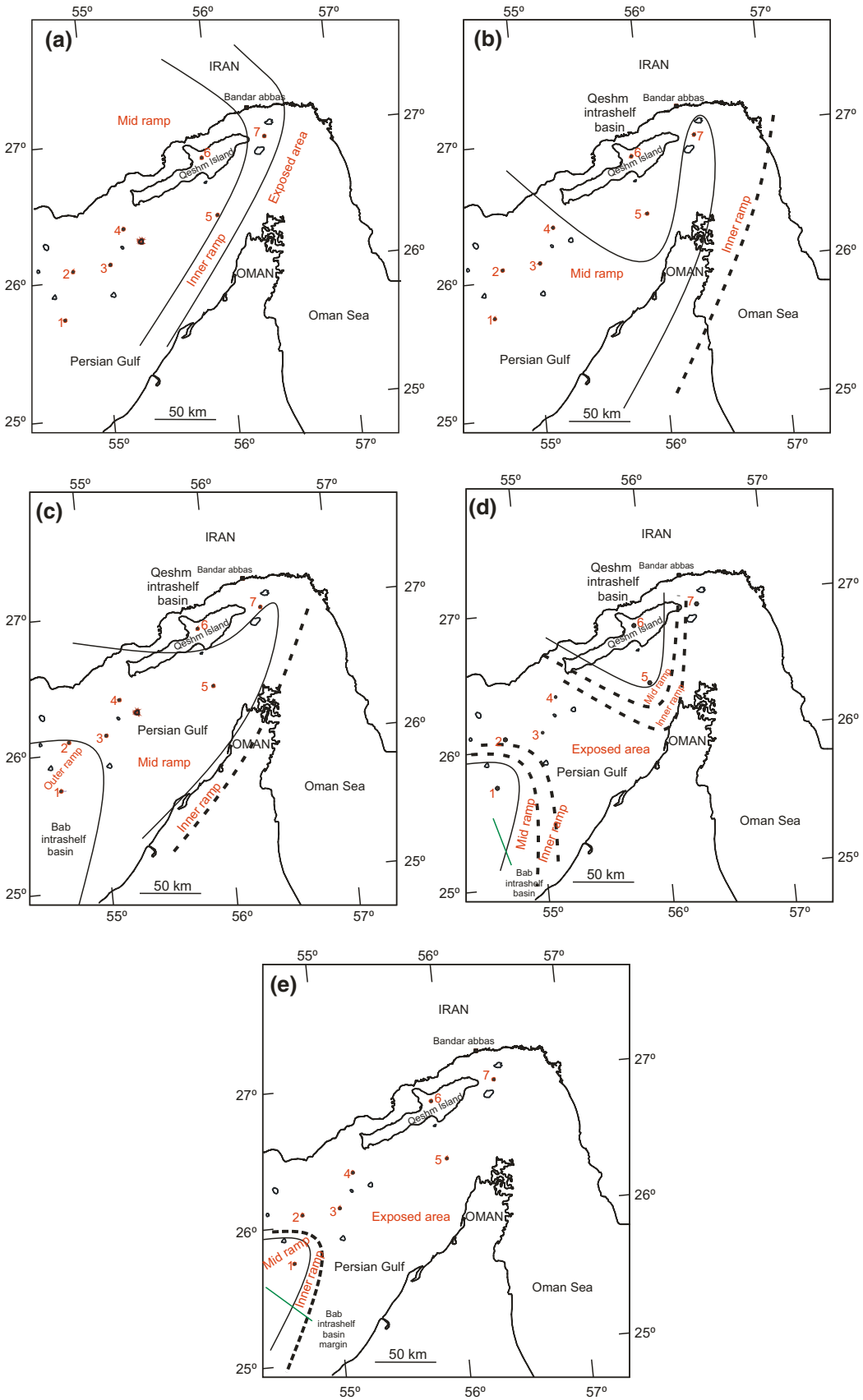

Fig. 14 Paleogeographic map of Aptian time in Qeshm island and offshore during the maximum flooding surface of Apt 1 (**a**), Apt 2 (**b**), Apt 3 (**c**), Apt 4 (**d**), and Apt 5 (**e**) sequences based on studied wells 1–7

8 Conclusion

The Dariyan Formation in Qeshm Island and offshore (southern Iran and the eastern part of Persian Gulf) is equivalent with the Hawar Member and Shu'aiba Formation of the Arabian Plate and contains 14 carbonate lithofacies which deposited on a carbonate ramp system. Sequence stratigraphic studies resulted in recognition of 5 Aptian third-order sequences toward Bab Basin (SW—well 1) and 4 Aptian third-order sequences toward Qeshm Island (NE wells 5 and 6). Toward wells 1, 5, and 6, a typical long-lasting transition from carbonate platform to intrashelf basin has been identified. The present of higher gamma ray peaks as maximum flooding surfaces in Apt 2–Apt 4 indicates that there might be a good source rock similar to the Arabian Platform. We interpret that salt movement, crustal warping, and basement fault reactivations were probably responsible for creation of an intrashelf basin in Qeshm Island and offshore. On the other hand, rudist and coral rudstone lithofacies, which probably have good reservoir properties, were deposited mid-ramp during deposition of Apt 3 (wells 2–4, 7 and partly in well 1) and Apt 4 (wells 1, 5, and 6) sequences. The Dariyan Formation around Qeshm Island mainly deposited in an intrashelf basin and should be considered as a new intrashelf basin in future Aptian paleogeographic maps.

Acknowledgments The authors would like to thank the National Iranian Oil Company, Exploration Directorate, for the support of this research. We also thank the Department of Geology at Ferdowsi University of Mashhad for their support.

References

Ainsworth RB. Sequence stratigraphic-based analysis of reservoir connectivity: influence of sealing faults—a case study from a marginal marine depositional setting. Petrol Geosci. 2006;12(2):127–41.

Ala MA. Salt diapirism in southern Iran. AAPG Bull. 1974;58(9):1758–70.

Alavi M. Regional stratigraphy of the Zagros fold-thrust belt of Iran and its proforeland evolution. Am J Sci. 2004;304:1–20.

Alavi M. Structures of the Zagros fold-thrust belt in Iran. Am J Sci. 2007;307(9):1064–95.

Al-Ghamdi N, Read FJ. Facies-based sequence stratigraphic framework of the Lower Cretaceous rudist platform, Shu'aiba Formation, Saudi Arabia. In: Van Buchem FSP, Al-Husseini MI, Maurer F, Droste HJ, editors. Barremian–Aptian stratigraphy and hydrocarbon habitat of the eastern Arabian Plate, vol. 1. GeoArabia Special Publication 4. Bahrain: Gulf PetroLink; 2010. p. 367–410.

Al-Husseini MI, Matthews RK. Tuning Late Barremian – Aptian Arabian Plate and global sequences with orbital periods. In: Van Buchem FSP, Al-Husseini MI, Maurer F, Droste HJ, editors. Barremian–Aptian stratigraphy and hydrocarbon habitat of the eastern Arabian Plate, vol. 1. GeoArabia Special Publication 4. Bahrain: Gulf PetroLink; 2010. p. 199–228.

Ali MY, Watts AB, Searle MP. Seismic stratigraphy and subsidence history of the United Arab Emirates (UAE) rifted margin and overlying foreland basins. In: Al Hosani K, Roure F, Ellison R, Lokier S, editors. Lithosphere dynamics and sedimentary basins: The Arabian Plate and analogues, frontiers in Earth sciences. Berlin: Springer; 2013. p. 127–43.

Alsharhan AS, Nairn AEM. Sedimentary basins and petroleum geology of the Middle East. Amsterdam: Elsevier; 1997.

Amthor JE, Kerans C, Gauthier P. Reservoir characterisation of a Shu'aiba carbonate ramp-margin field, northern Oman. In: Van Buchem FSP, Al-Husseini MI, Maurer F, Droste HJ, editors. Barremian–Aptian stratigraphy and hydrocarbon habitat of the eastern Arabian Plate, vol. 2. GeoArabia Special Publication 4. Bahrain: Gulf PetroLink; 2010. p. 549–76.

Azimi R. Biostratigraphy, micropalaeontology and micropaleontological studies on the cutting and core samples of drilled sequence of well 5. Report 1801. Tehran: Exploration Directorate of National Iranian Oil Company; 2010a.

Azimi R. Biostratigraphy, micropalaeontology and micropaleontological studies on the cutting and core samples of drilled sequence of well 7. Report 1808. Tehran: Exploration Directorate of National Iranian Oil Company; 2010b.

Bahroudi A, Koyi HA. Tectono-sedimentary framework of the Gachsaran Formation in the Zagros foreland basin. Mar Petrol Geol. 2004;21(10):1295–310.

Bechennec F, Le Metour J, Rabu D, et al. The Hawasina Nappes; stratigraphy, palaeogeography and structural evolution of a fragment of the South-Tethyan passive continental margin. Geol Soc Spec Publ. 1990;49:213–23.

Berberian M, King GCP. Towards a paleogeography and tectonic evolution of Iran. Can J Earth Sci. 1981;18(2):210–65.

Boote DRD, Mou D. Safah field, Oman: retrospective of a new-concept exploration play, 1980 to 2000. GeoArabia. 2003;8(3):367–430.

Droste HJ. Sequence-stratigraphic framework of the Aptian Shu'aiba formation in the Sultanate of Oman. In: Van Buchem FSP, Al-Husseini MI, Maurer F, et al., editors. Barremian-Aptian stratigraphy and hydrocarbon habitat of the eastern Arabian Plate, vol. 1. GeoArabia Special Publication 4. Bahrain: Gulf PetroLink; 2010. p. 229–83.

Dunham RJ. Classification of carbonate rocks according to depositional textures. In: Ham WE, editor. Classification of carbonate rocks, vol. 1. AAPG Memoir; 1962. p. 108–21.

Edgell HS. Salt tectonism in the Persian Gulf basin. Geol Soc London Spec Publ. 1996;100(1):129–51.

Ehrenberg SN, Svånå TA. Use of spectral gamma-ray signature to interpret stratigraphic surfaces in carbonate strata: an example from the finnmark carbonate platform (Carboniferous-Permian), Barents Sea. AAPG Bull. 2001;85(2):295–308.

Embry AF, Klovan JE. A Late Devonian reef tract on north-eastern Banks Island, Northwest Territories. Bull Can Petrol Geol. 1971;19:730–81.

Flugel E. Microfacies of carbonate rocks: analysis, interpretation and application. New York: Springer; 2010.

Fonooni B. Biostratigraphy, micropalaeontology and micropaleontological studies on the cutting and core samples of drilled sequence of well 1. Report 1788. Tehran: Exploration Directorate, National Iranian Oil Company; 2010.

Glennie KW. Cretaceous tectonic evolution of Arabia's eastern plate margin: a tale of two oceans. SEPM Spec Publ. 2000;69:9–20.

Granier B. Holostratigraphy of the Kahmah regional series in Oman. Qatar and the United Arab Emirates: Notebooks of Geology; 2008.

Granier B, Al Suwaidi AS, Busnardo R, et al. New insight on the stratigraphy of the "Upper Thamama" in offshore Abu Dhabi (UAE), vol. 5. Qatar and the United Arab Emirates: Notebooks of Geology; 2003.

Hadavandkhani N. Biostratigraphy, micropalaeontology and micropaleontological studies on the cutting and core samples of drilled sequence of well 2. Report 1807. Tehran: Exploration Directorate, National Iranian Oil Company; 2010.

Halfar J, Ingle JC. Modern warm-temperate and subtropical shallow-water benthic foraminifera of the southern Gulf of California, Mexico. J Foramin Res. 2003;33(4):309–29.

Herrle JO, Mutterlose J. Calcareous nannofossils from the Aptian–Early Albian of SE France: paleoecological and biostratigraphic implications. Cretaceous Res. 2003;24:1–22.

Hillgärtner H. Anatomy of a microbially constructed, high-energy, ocean-facing carbonate platform margin (earliest Aptian, northern Oman Mountains). In: Van Buchem FSP, Al-Husseini MI, Maurer F, et al., editors. Barremian–Aptian stratigraphy and hydrocarbon habitat of the eastern Arabian Plate, vol. 1. GeoArabia Special Publication 4. Bahrain: Gulf PetroLink; 2010. p. 285–300.

Hillgärtner H, Van Buchem F, Gaumet F, et al. The Barremian–Aptian evolution of the eastern Arabian carbonate platform margin (northern Oman). J Sediment Res. 2003;73(5):756–73.

Hughes GW. Bioecostratigraphy of the Shu'aiba Formation, Shaybah field. Saudi Arabia. GeoArabia. 2000;5(4):545–78.

Hughes GW. Middle to Upper Jurassic Saudi Arabian carbonate petroleum reservoirs: biostratigraphy, micropalaeontology and palaeoenvironments. GeoArabia. 2004;9:79–114.

Hughes GW. Complex-walled agglutinated foraminiferal biostratigraphy and palaeoenvironmental significance from the Jurassic supercycle-associated carbonates of Saudi Arabia. In: Abstracts 7th international workshop Agglutinated Foraminifera, Urbino, Italy; 2005. p. 19–20.

Immenhauser A, Hillgärtner H, Sattler U, et al. Barremian-Lower Aptian Qishn Formation, Haushi-Huqf area, Oman: a new outcrop analogue for the Kharaib/Shu'aiba reservoirs. GeoArabia. 2004;9(1):153–94.

Immenhauser A, Hillgärtner H, Van Bentum EC. Microbial-foraminiferal episodes in the Early Aptian of the southern Tethyan margin: ecological significance and possible relation to oceanic anoxic event 1a. Sedimentology. 2005;52:77–99.

Immenhauser A, Schlager W, Burns SJ, et al. Late Aptian to Late Albian sea level fluctuations constrained by geochemical and biological evidence (Nahr Umr Formation, Oman). J Sediment Res. 1999;69:434–66.

Jahani S, Callot JP, Frizon de Lamotte D, et al. The salt diapirs of the Eastern Fars Province (Zagros, Iran): A brief outline of their past and present. In: Lacombe O, Lavé J, Roure F, Vergés, J, editors. Thrust belts and foreland basin: from fold kinematics to hydrocarbon systems. Berlin: Springer; 2007. p. 289–308.

Jalali MR. Paleolog chart of well 6. Tehran: Exploration Directorate, National Iranian Oil Company; 1969.

James GA, Wynd JG. Stratigraphic nomenclature of Iranian oil consortium agreement area. AAPG Bulletin. 1965;49(12):2182–245.

Konyuhov AI, Maleki B. The Persian Gulf Basin: geological history, sedimentary formations, and petroleum potential. Lithol Miner Resour. 2006;41(4):344–61.

Masse JP, Borgomano J, Al-Maskiry S. Stratigraphy and tectonosedimentary evolution of a Late Aptian-Albian carbonate margin: the northeastern Jebel Akhdar (Sultanate of Oman). Sediment Geol. 1997;113:269–80.

Maurer F, Al-Mehsin K, Pierson BJ, et al. Facies characteristics and architecture of Upper Aptian Shu'aiba clinoforms in Abu Dhabi. In: Van Buchem FSP, Al-Husseini MI, Maurer F, et al., editors. Barremian–Aptian stratigraphy and hydrocarbon habitat of the eastern Arabian Plate, vol. 2. GeoArabia Special Publication 4. Bahrain: Gulf PetroLink. 2010. p. 445–68.

Meyer M. Le complexe récifal kimméridgien-tithonien du Jura meridional interne (France), évolution multifactorielle, stratigraphie et tectonique. Terre & Environment; 2000. p. 24.

Motiei H. Stratigraphy of the Zagros. Geological Survey of Iran (in Persian language): Treatise on the Geology of Iran; 1993.

Motiei H. Petroleum Geology of Zagros, 1 and 2. Geological Survey of Iran Publications (in Persian language); 1995.

Motiei H. Simplified table of rock unit in southwest Iran (a map unpublished, KEPS Company); 2001.

Mutterlose J, Bornemann A, Herrle J. The Aptian-Albian cold snap: evidence for "mid" Cretaceous icehouse interludes. Neues Jahrb Geol P-A. 2009;252(2):217–25.

Nayebi Z. Biostratigraphy, micropalaeontology and micropaleontological studies on the cutting and core samples of drilled sequence of well 3. Report 1174, Exploration Directorate, National Iranian Oil Company; 2000.

Nayebi Z. Biostratigraphy, micropalaeontology and micropaleontological studies on the cutting and core samples of drilled sequence of well 4. Report 517, Exploration Directorate, National Iranian Oil Company; 2001.

Ogg JG, Agterberg FP, Gradstein FM. The Cretaceous Period. In: Gradstein F, Ogg J, Smith A, editors. A Geological Time Scale 2004. Cambridge University Press; 2004.

Pierson BJ, Eberli GP, Al-Mehsin K, et al. Seismic stratigraphy and depositional history of the Upper Shu'aiba (Late Aptian) in the UAE and Oman. In: Van Buchem FSP, Al-Husseini MI, Maurer F, et al., editors. Barremian–Aptian stratigraphy and hydrocarbon habitat of the eastern Arabian Plate. GeoArabia Special Publication 4, Gulf PetroLink, Bahrain. 2010. 2. p. 411–4.

Piryaei A, Reijmer JJG, Borgomano J, et al. Late Cretaceous tectonic and sedimentary evolution of the Bandar Abbas area, Fars region. Southern Iran. J Petrol Geol. 2011;34(2):157–80.

Pittet B, Van Buchem FSP, Hillgärtner H, et al. Ecological succession, palaeoenvironmental change, and depositional sequences of Barremian-Aptian shallow water carbonates in northern Oman. Sedimentology. 2002;49(3):555–81.

Rameil N, Immenhauser A, Warrlich G, et al. Morphological patterns of Aptian Lithocodium–Bacinella geobodies: relation to environment and scale. Sedimentology. 2010;57(3):883–911.

Raven MJ, Van Buchem FSP, Larsen PH, et al. Late Aptian incised valleys and siliciclastic infill at the top of the Shu'aiba Formation (Block 5, offshore Qatar). In: Van Buchem FSP, Al-Husseini MI, Maurer F, et al., editors. Barremian–Aptian stratigraphy and hydrocarbon habitat of the eastern Arabian Plate. GeoArabia Special Publication 4, Gulf PetroLink, Bahrain. 2010. 2. p. 469–502.

Ruban DA, Al-Husseini MI, Iwasaki Y. Review of Middle East Paleozoic plate tectonics. GeoArabia. 2007;12:35–55.

Sadooni FN. Stratigraphic sequence, microfacies and petroleum prospectus of the Yamama Formation. Lower Cretaceous, southern Iraq, AAPG Bull. 1993;77(11):1971–88.

Schroeder R, Van Buchem FSP, Cherchi A, et al. Revised orbitolinid biostratigraphic zonation for the Barremian–Aptian of the eastern Arabian Plate and implications for regional stratigraphic correlations. In: Van Buchem FSP, Al-Husseini MI, Maurer F, et al., editors. Barremian–Aptian stratigraphy and hydrocarbon habitat of the eastern Arabian Plate. GeoArabia Special Publication 4, Gulf PetroLink, Bahrain. 2010. 1. p. 49–96.

Scott RW, Simo JAT, Masse JP. Economic resources in Cretaceous carbonate platforms: An Overview: Chapter 2. In: Simo JAT, Scott RW, Masse JP, editors. Cretaceous carbonate platforms, AAPG Memoir. 1993; 56:15–23.

Sharland PR, Archer R, Casey DM, et al. Arabian Plate Sequence Stratigraphy. GeoArabia Special Publication 2, Gulf PetroLink, Bahrain; 2001.

Simmons MD, Whittaker JE, Jones RW. Orbitolinids from Cretaceous sediments of the Middle East—A revision of the Henson, F.R.S. and Associates Collection. In: Hart MB, Kaminski MA, Smart CW, editors. Proceedings of the fifth international workshop on agglutinated foraminifera, vol. 7. Grzybowski Found Special Publication; 2000. p. 411–37.

Strohmenger CJ, Steuber T, Ghani A, et al. Sedimentology and chemostratigraphy of the Hawar and Shu'aiba depositional sequences, Abu Dhabi, United Arab Emirates. In: Van Buchem FSP, Al-Husseini MI, Maurer F, et al., editors. Barremian-Aptian stratigraphy and hydrocarbon habitat of the eastern Arabian Plate, vol. 2. Geo Arabia Special Publication 4. Bahrain: Gulf PetroLink; 2010. p. 341–65.

Vahrenkamp VC. Chemostratigraphy of the Lower Cretaceous Shu'aiba Formation: A $\delta^{13}C$ reference profile for the Aptian Stage from the southern Neo-Tethys Ocean. In: Van Buchem FSP, Al-Husseini MI, Maurer F, et al., editors. Barremian–Aptian stratigraphy and hydrocarbon habitat of the eastern Arabian Plate, vol. 1. GeoArabia Special Publication 4. Bahrain: Gulf PetroLink; 2010. p. 107–37.

Van Buchem FSP, Pittet B, Hillgartner H, et al. High-resolution sequence stratigraphic architecture of Barremian/Aptian carbonate systems in Northern Oman and the United Arab Emirates (Khairab and Shuaiba Formations). GeoArabia. 2002;7:461–500.

Van Buchem FSP, Al-Husseini MI, Maurer F, et al. Sequence stratigraphic synthesis of the Barremian–Aptian of the eastern Arabian Plate and implications for the petroleum habitat, vol. 1. GeoArabia Special Publication 4. Bahrain: Gulf PerrLlink; 2010a. p. 9–48.

Van Buchem FSP, Baghbani D, Bulot LG, et al. Barremian–Lower Albian sequence stratigraphy of southwest Iran (Gadvan, Dariyan and Kazhdumi formations) and its comparison with Oman, Qatar and the United Arab Emirates. In: Van Buchem FSP, Al-Husseini MI, Maurer F, et al., editors. Barremian–Aptian stratigraphy and hydrocarbon habitat of the eastern Arabian Plate, vol. 2. GeoArabia Special Publication 4. Bahrain: Gulf PetroLink; 2010b. p. 503–48.

Van Wagoner JC, Posamentier HW, Mitchum RMJ, et al. An overview of the fundamentals of sequence stratigraphy and key definitions. Sea-level changes: an integrated approach, vol. 42. Tulsa: Society of Economic Paleontologists and Mineralogists Special Publication; 1988, p. 39–45.

Vilas L, Masse JP, Arias C. Orbitolina episodes in carbonate platform evolution: the Early Aptian model from SE Spain. Palaeogeogr Palaeocl. 1995;119:35–45.

Vincent, B., Van Buchem FSP, Bulot LG, et al. Carbon-isotope stratigraphy, biostratigraphy and organic matter distribution in the Aptian–Lower Albian successions of southwest Iran (Dariyan and Kazhdumi formations). In: van Buchem FSP, Al-Husseini MI, Maurer F, et al., editors. Barremian–Aptian stratigraphy and hydrocarbon habitat of the eastern Arabian Plate, vol. 1. GeoArabia Special Publication 4. Bahrain: Gulf PetroLink; 2010. p. 139–97.

Weissert H, Lini A. Ice age interludes during the time of Cretaceous Greenhouse Climate? In: Mueller, DW, McKenzie JA, Weissert H, editors. Controversies in modern geology. London: Academic Press; 1991. p. 173–91.

Wignall PB, Myers KJ. Interpreting benthic oxygen levels in mudrocks: a new approach. Geology. 1988;16:452–5.

Wilson JL. Carbonate facies in geologic history. Berlin: Springer; 1975.

Witt W, Gökdağ H. Orbitolinid biostratigraphy of the Shu'aiba Formation (Aptian), Oman, implications for reservoir development. In: Simmons MD, editor. Micropalaeontology and hydrocarbon exploration in the Middle East. Chapman and Hall: London; 1994. p. 221–42.

Yose LA, Ruf AS, Strohmenger CJ, et al. Three dimensional characterization of a heterogeneous carbonate reservoir, Lower Cretaceous, Abu Dhabi (United Arab Emirates). In: Harris PM, Weber LJ, editors. Giant hydrocarbon reservoirs of the world: from rock to reservoir characterization and modeling. AAPG Memoir 88/Society of Economic Paleontologists and Mineralogists Special Publication; 2006. p. 173–212.

Yose LA, Strohmenger CJ, Al-Hosani I, et al. Sequence stratigraphic evolution of an Aptian carbonate platform (Shu'aiba Formation), eastern Arabian Plate, onshore Abu Dhabi, United Arab Emirates. In: Van Buchem FSP, Al-Husseini MI, Maurer F, et al., editors. Barremian–Aptian stratigraphy and hydrocarbon habitat of the eastern Arabian Plate, vol. 2. GeoArabia Special Publication 4. Bahrain: Gulf PetroLink; 2010. p. 309–40.